Asian Journal of Chemistry; Vol. 36, No. 9 (2024), 2038-2044

ASIAN JOURNAL OF CHEMISTRY

https://doi.org/10.14233/ajchem.2024.32033

Physico-chemical Studies of Alkali-Free MgAl Layered Double Hydroxide for Electrolyte Conductivity Studies at Ambient Temperature

MUHAMAD SYAFIQ ZAINUDIN ITHNIN[1], NAZRIZAWATI AHMAD TAJUDDIN[1,*] and HUSSEIN HANIBAH[2]

[1]Faculty of Applied Sciences, Universiti Teknologi MARA, 40450 Shah Alam, Selangor, Malaysia
[2]Centre of Foundation Studies, Universiti Teknologi MARA, Cawangan Selangor, Kampus Dengkil, 43800 Dengkil, Selangor, Malaysia

*Corresponding author: E-mail: nazriza@uitm.edu.my

Received: 27 May 2024; *Accepted*: 2 July 2024; *Published online*: 30 August 2024; AJC-21728

The current work reports the physico-chemical properties of MgAl layered double hydroxide (LDH), which was synthesized *via* alkali free co-precipitation method with ratio of 4:1 and further calcined at 450 ºC for 13 h. The correlation of crystallinity, morphology and particle size of MgAl LDH before and after calcined were examined using thermogravimetric analysis (TGA), powder X-ray diffraction (PXRD), Brunaeur-Emmette-Teller (BET), Fourier transform infrared (FTIR) and field emission scanning electron microscope (FESEM). The conductivity study of calcined MgAl LDH was measured using an AC conductivity meter, which reveals the optimum concentration of MgAl LDH with an electrolytic conductivity (κ) of 0.1256 µS/cm at 25 ºC. This concentration was further used in the remaining electrolyte system in the presence of lithium perchlorate ($LiClO_4$). The κ values was measured at various C_{salt} (10^{-8}–10^{-3} mol cm^{-3}) and the limiting molar conductivity (Λ_o) values was also determined using power law.

Keywords: MgAl LDH, Hydrotalcite, Layer double hydroxide, Limiting molar conductivity, Power law.

INTRODUCTION

The development of efficient and good solutions for storing energy, such as secondary battery systems, has received great attention from researchers globally. Batteries, in general, are a promising energy storage technology for integrating renewable resources that provide alternating electricity to the grid [1]. Since the first commercialization of lithium ion batteries in 1991, their progress has piqued researchers' interest and resulted in a wide range of applications [2]. Currently, different types of polymers, dopants of inorganic salts and the addition of nanocomposite materials are seen to be the most likely answers in the creation of new and improved power sources in battery technology [3,4].

Despite their widespread use in battery technology, no material combination has yet achieved the optimal polymer electrolyte (PE) solution. Most of this combination results in an extremely low ionic conductivity (κ) (~10^{-6} S cm^{-1}) at the ambient temperature, which remains below the level of performance required for many applications (~10^{-3} S cm^{-1}), severely limiting battery power [5,6]. Furthermore, a clear mechanism underlying this low conductivity value remains unknown, particularly in solid polymer electrolyte (SPE) systems due to the complexity of the coexisting amorphous and crystalline phases [7]. However, the usage of nanocomposites as a filler in electrolyte system is said to enhance the degree of salt dissociation (α) [8] and increase the total free moving ions in the electrolyte system [9,10].

Layered double hydroxides (LDHs), also known as hydrotalcite, are the anionic clays with high absorption capabilities and a structure similar to brucite ($Mg(OH)_2$) [11]. In general, LDH consists of brucite-like layers where some divalent and trivalent cations have been substituted, resulting in positively charged layers balanced by anions between the layers [12-14]. The gap between the layers also contains water molecules [15]. The general equation for the composition of LDH is as follows:

$$[M^{2+}_{1-x}M^{3+}_{x}(OH)_2(A^{n-})_{x/n}]\cdot mH_2O$$

where M^{2+} and M^{3+} are bivalent and trivalent metal cations, respectively and A^{n-} is the interlayer anion [11,16].

LDHs can be synthesized utilizing a variety of techniques, including sol-gel, ion exchange and hydrothermal treatment,

with co-precipitation being the most reliable and straightforward way [17]. However, numerous parameters during the synthesis process can be used to customize the characteristics, such as modifying the metals in the inorganic layer or the inorganic or organic anions between the inorganic layers [16]. The adaptability of the LDH's structure provides it with unique qualities which can be applied in a variety of situations.

Until now, several applications of LDHs have been documented, including catalysts and their support, electrodes, adsorbents/ion exchangers and drug carriers [18-20]. Furthermore, LDHs are the best fillers for polymer nanocomposites since they do not have the problems that clay minerals possess [21]. Efforts have been undertaken to maximize material performance by altering both the composition and particle shape of LDHs. According to Wijitwongwan *et al*. [18], the particle size and size distribution can have a substantial impact on material performance due to surface area, packing density, flowability, dissolution rate and optical characteristics.

In this study, magnesium aluminium layered double hydroxide (MgAl LDH) was synthesized *via* alkali free co-precipitation method with a ratio of 4:1 correspond to magnesium and aluminium, respectively. This method is the predominant technique for synthesizing LDHs, which involves a solution containing mixed alkali soda and mixed salts solution. The product of MgAl LDH was further characterized by various physicochemical techniques. Calcined MgAl LDH has been chosen for further characterized on conductivity due to the beneficial properties obtained from the calcination process.

EXPERIMENTAL

Magnesium(II) nitrate hexahydrate ($Mg(NO_3)_2{\cdot}6H_2O$) and ammonium nitrate (NH_4NO_3) were obtained from Systerm Chemicals, Malaysia. Aluminum(III) nitrate nonahydrate ($Al(NO_3)_3{\cdot}9H_2O$) and ammonium hydroxide solution were obtained from R&M Chemicals. The inorganic salt anhydrous $LiClO_4$ with purity ≥ 98% was obtained from Fluka (Sigma-Aldrich). High-performance liquid chromatography (HPLC) grade of acetonitrile (Fisher-Scientific) with purity ≥ 99.9% was obtained from Alfa Laboratori Sdn Bhd, Malaysia. All the chemicals were used without any further purification in this research.

Preparatrion of MgAl LDH *via* co-precipitation method: An alkali free co-precipitation method was used to synthesize MgAl LDH with molar ratio of 4:1. The synthesis was prepared by mixing an aqueous solution of metallic cations (solution A) with a nitrate solution (solution B) simultaneously dropwise under vigorous stirring at pH 8.5. Ammonium hydroxide solution was added dropwise to maintain the pH. Solution A was prepared by mixing 1 M $Mg(NO_3)_2{\cdot}6H_2O$ with 1 M $Al(NO_3)_3{\cdot}9H_2O$ according to 4:1 MgAl molar ratio to make up 100 mL solution. Solution B consisted of 2 M $(NH_4)_2CO_3$ in 100 mL of distilled water. The co-precipitation product was brought to reflux for 24 h before being aged at 65 ºC. Then, the solution was filtered and rinsed with distilled water until the pH reached 7. The precursor was placed in an oven at 100 ºC for 24 h followed by calcination at 450 ºC for 13 h.

Preparation of MgAl LDH solution: The MgAl LDH solution were prepared by dissolving the LDH in acetonitrile to obtain a range of MgAl LDH solutions with percent ratios ranging from 0.2 to 10.0 % (w/v) as shown in Table-1. A sufficient amount of MgAl LDH was weighted and transferred to a beaker containing an appropriate amount of acetonitrile as solvent. The mixture was then stirred on a hot plate magnetic stirrer at 50 ºC for 24 h. The solution was then allowed to cool to room temperature before use. Similar procedures were taken to prepare different ratio of MgAl LDH stock solutions. The conductivity measurement was performed to determine the ratio that give the optimum ionic conductivity (κ). This solution was then used as a stock solution to prepare electrolyte solutions.

TABLE-1
DIFFERENT CONCENTRATIONS OF MgAl LDH IN ACETONITRILE

Percent ratio (w/v)	Volume of acetonitrile (mL)	Mass (g)	Actual mass (g)
0.20	50	0.10	0.1005
0.40	50	0.20	0.2012
0.60	50	0.30	0.3019
0.80	50	0.40	0.4023
1.00	50	0.50	0.5032
2.00	50	1.00	1.0034
4.00	50	2.00	2.0041
6.00	50	3.00	3.0059
8.00	50	4.00	4.0064
10.00	50	5.00	5.0072

Preparation of $LiClO_4$-MgAl LDH electrolyte solution: The $LiClO_4$-MgAl LDH electrolyte solution was prepared by dissolving $LiClO_4$ in MgAl LDH solution, which gives the optimum ionic conductivity (κ) value. Because of its lower lattice energy (723 kJ/mol) and its less hygroscopic behaviour, $LiClO_4$ has been selected, since it has a higher degree of dissociation. The stock solution of $LiClO_4$ in MgAl LDH solution with a concentration of about 1.00×10^{-4} mol cm^{-3} was also prepared. The electrolyte solution of $LiClO_4$ in MgAl LDH solution of known concentration was prepared by transferring a known amount of $LiClO_4$ salt into a solvent of fixed volume (MgAl LDH in acetonitrile). The electrolyte solution was stirred at 50 ºC for 24 h before further use and this solution was used as stock solution. Then, a series of dilution of the stock solution were prepared by adding MgAl LDH solution.

Characterization: Thermogravimetric analysis (TGA) of the as-synthesized MgAl LDH was carried out using Setaram model SETSYS Evolution TGA-DTA/DSC to observe the weight loss and evaluate the interlayer water and carbonate content. Sample was heated at 800 ºC with a heating rate of 10 ºC min^{-1} under nitrogen flow. Powder X-ray diffraction (PXRD) model PANanalytical X'pert PRO was operated to observed the sample structure. Measurements were made with diffraction angle 2θ from 8 to 85º at a speed of 1º min^{-1}. Fourier transform infrared spectroscopy (FTIR) model Perkin-Elmer Spectrum One was run to observe the bonding type and structural of MgAl LDH. The sample was mixed with KBr and compressed into a thin transparent pallet. Then, sample was scan and analyze from 0

to 4500 cm^{-1} with 2 cm^{-1} resolutions. The surface morphologies of the synthesized MgAl LDH were studied using field emission scanning electron microscope (FESEM) model JEOL JSM-7600F microscope with a Schottky emitter at an accelerating voltage of 2.0 kV with a beam current of 1.0 mA. The Brunauer-Emmett-Teller (BET) technique was used to analyze the surface area of MgAl LDH sample. Surface area and pore size distribution measurements were carried out using Quantachrome ChemBET 3000 chemisorption analyzer (Hook, United Kingdom). For conductivity measurements, the electrolytic conductivity (κ) of the solutions were measured at 25 ºC using Mettler Toledo SevenCompact S230 conductivity meter (Schwerzenbach, Switzerland) with its AC dip-type conductivity probe InLab® 731 (measuring range 0.01-1000 mS cm^{-1}) and InLab® 741 (measuring range 0.001-500 μS cm^{-1}).

RESULTS AND DISCUSSION

Thermal studies: The thermogram (TGA) of the prepared LDH and MgAl LDH is shown in Fig. 1. This investigation has been accomplished in order to determine the appropriate temperature for decomposition, which is required in order to calcine the sample further. In this study, MgAl LDH sample has undergone several stages of weight losses and lost about 45.58%, which is approximately 4.56 mg of its initial weight upon heating to 800 ºC. The first weight loss occurred between 20 and 240 ºC due to the removal of physically adsorbed and interlayer water molecules present in the material. During this phase, which is also called the dehydration process, the structure of the layered MgAl remains unchanged. For the second stage of weight loss, it was observed in the DTG curve at 240 ºC up to 530 ºC. These losses correspond to the dihydroxylation of hydroxyl group (OH^-) anions and the decomposition of the interlayer carbonates anions into carbon dioxide and oxide (O^{2-}) ions, which also known as decarbonation and decarboxylation. According to Smolakova *et al.* [22], the weight loss was originated from H_2O, CO_2, NO and NH_3 removal due to the dihydroxylation and the decomposition of carbonates in the interlayer. The last weight loss up to 800 ºC, is attributed to the removal of the remaining carbonaceous material and formation of metal oxides. From the result, it can be concluded that the suitable temperature for further calcine the sample is above 240 ºC. Table-2 summarizes the decomposition of MgAl LDH measured by thermal studies.

XRD studies: The layered structure of neat and calcined MgAl LDH were confirmed *via* PXRD patterns as in Fig. 2. The sharp, intensive and symmetric peaks displayed in the PXRD diffraction pattern give an indication of highly crystalline nature in the synthesis of LDHs-precursor [13]. All peaks assigned to the planes confirmed that the neat MgAl LDH was successfully synthesized. The peaks assigned to (003), (006), (009), (012), (015), (018), (110) and (113) planes with reflection at 2θ = 11.5º, 23.2º, 30.7º, 34.7º, 39.2º, 46.7º, 60.6º

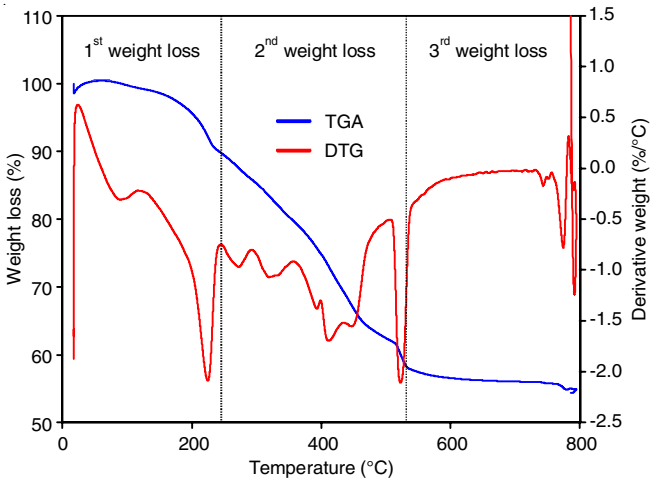

Fig. 1. TGA-DTG curves of MgAl LDH

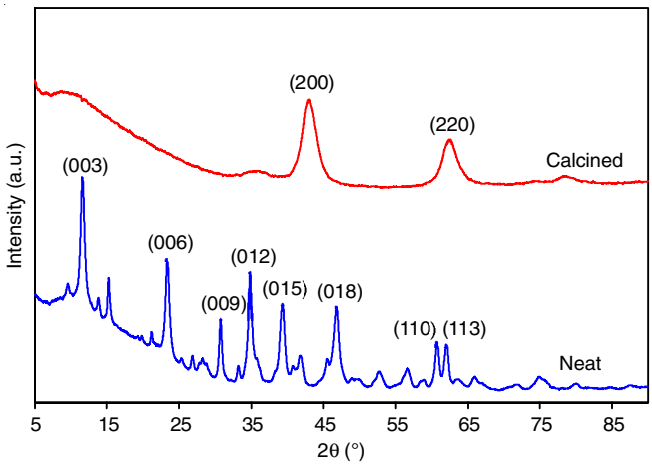

Fig. 2. PXRD pattern of neat and calcined MgAl LDH

and 62.0º (JCPDS card No. 14-0191), respectively, reveal the formation of a characteristic hexagonal LDH lattice with rhombohedral symmetry of crystalline hydrotalcite-like LDHs. The (110) and (113) diffraction peaks at 2θ = 60.6º and 62.0º, respectively suggest a uniform dispersion of Mg^{2+} and Al^{3+} metal cations in brucite-like layers. These findings are in good agreement with the reported literature [23-25].

After the calcination process, the thermal decomposition of hydrotalcite precursor led to the disappearance of MgAl LDH diffraction peaks and resulting in the formation of mixed oxide phase corresponding to MgO and AlO structures. It can be shown with the disappearance of the main basal reflections of (003), (006) and (009). As a result, formation of two intensive peaks and characteristic diffraction at 2θ = 43.3º and 62.4º that correspond to the mixed Mg-Al oxides (MgO and AlO) were clearly observed, which can be indexed to (200) and (220) respectively (JCPDS card No. 45-0946). This can be explained by the destruction of LDHs brucite layer (dehydration, dihydro-

TABLE-2
DECOMPOSITION TEMPERATURE OF MgAl LDH

Sample	Decomposition temperature (°C)	1st weight loss (°C) (dehydration)	2nd weight loss (°C) (dehydroxylation)	3rd weight loss (°C) (decarboxylation/decarbonation)
Neat MgAl LDH	20-800	20-240	240-530	530-800

xylation, decarbonation) and the formation of mixed oxide during calcination at 450 ºC [13]. Table-3 shows the textural properties of d-spacing and lattice parameter of neat and calcined MgAl LDH.

TABLE-3
TEXTURAL PROPERTIES OF D SPACING AND LATTICE PARAMETER OF MgAl LDH

Materials	d spacing (Å)	Lattice parameter (Å)	
		a	c
Neat MgAl LDH	1.71	10.54	10.54
Calcined MgAl LDH	1.315	4.22	4.22

FTIR studies: The FTIR spectra of MgAl LDH before and after calcination have been studied and shown in Fig. 3. The characteristic absorption has been showed at peak 3446 cm^{-1}, which can be assigned to the stretching vibration mode of O-H functional group, arising from interlayer water molecules and the hydroxyl groups present on the surface as well as in the brucite-like layers of the LDH [26]. The peaks at 1484, 1423 and 1364 cm^{-1} exist due to carbonate content in the sample and can be assigned to the stretching and bending vibration of carbonate species [27]. All the absorption bands below 1000 cm^{-1} are associated to the lattice vibration of metal oxides (M-O, O-M-O and M-O-M) stretching modes in the brucite-like layer, where M stands for Mg^{2+} and Al^{3+} cations [28]. Thus, the absorption peaks at 796, 686 and 599 cm^{-1} can be attribute to the metal oxide stretching modes.

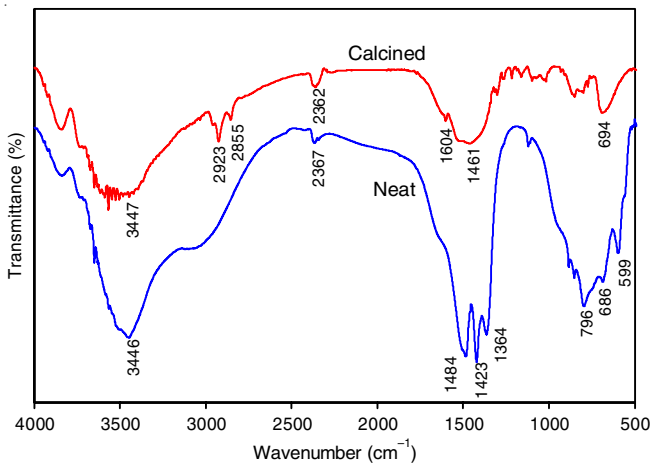

Fig. 3. FTIR spectra of MgAl LDH before and after calcined

After calcination, the spectra show less intensity compared to the uncalcined spectra. There is a peak appeared at 1604 cm^{-1}, which indicate the vibration of O-H bending vibration of the interlayer water molecule. This peak might be appeared due to the improper storage of MgAl LDH or that water in air was absorbed after calcination [29]. Since LDH is very sensitive to moisture, thus it must be kept properly to avoid absorption of moisture. Table-4 summarized the key IR adsorption band presence in neat and calcined MgAl LDH.

Morphological studies: Before calcination (Fig. 4a), it is observed that MgAl LDH is composed of non-uniform platelets

TABLE-4
KEY IR ABSORPTION BANDS (cm^{-1}) PRESENCE IN NEAT AND CALCINED MgAl LDH

Materials	Characteristic band	Wavenumber (this study)	Wavenumber (reported)	Ref.
Neat MgAl LDH	O–H stretching	3446	3700-3000	[30]
	C–O stretching	1484, 1423, 1364	1540-1350	[27]
	Mg–O/Al–O stretching	796, 686, 599	770-550	[26]
Calcined MgAl LDH	O–H stretching	3447	3443	[31]
	O–H bending	1604	1640	[32]
	C–O stretching	1461	1400	[29]
	Mg–O/Al–O stretching	694	700-680	[32]

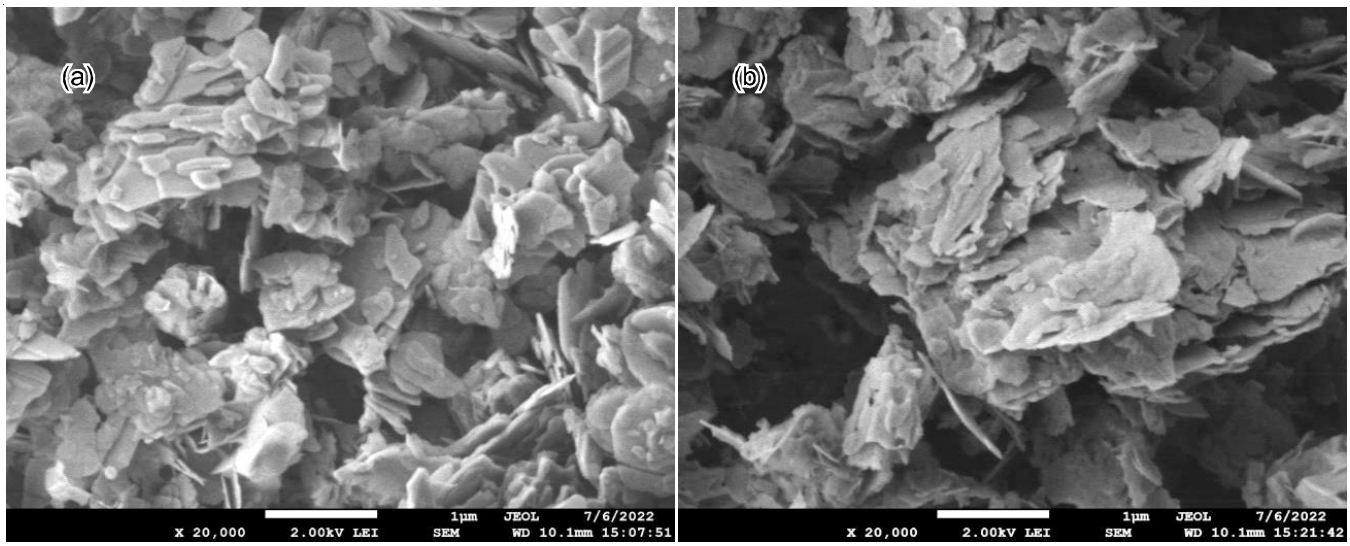

Fig. 4. SEM micrographs of (a) neat MgAl LDH and (b) calcined MgAl LDH

and aggregates of nanoparticles can be observed based on the compact sand rosses shaped observed in the image. The possible reason is that the structure was formed with numerous fine nanoparticles [13]. After calcination (Fig. 4b) at 450 ºC, the compact structure was destroyed and change the structure due to the removal of hydroxyl groups in the metal hydroxide layers and from the releasing or decomposing of carbonate ion existed in the interlayer space as charge balancing anion during the calcination [23]. According to the reported findings, the preparation method significantly affects the morphology of the LDHs, resulting in solids that are hexagonal in shape, presence of platelets or dense agglomerates of the non-porous grains [13].

BET studies: The textural properties of LDH sample in this study have been characterized and calculated by using Brunauer-Emmet-Teller (BET) *via* N_2 gas adsorption and desorption technique. Nitrogen (adsorption and desorption isotherms at relative pressure range (0.01-1.00) were measured to study the pore size distribution and specific surface area of the MgAl LDH. The N_2 adsorption and desorption curve of neat and calcined MgAl LDH samples are illustrated in Fig. 5. It is clearly shown that the isotherm for both neat and calcined MgAl LDH may be classified as type IV isotherm according to IUPAC classification and its significant N_2 uptake at high relative pressure suggest that the materials may feature mesopores. Additionally, the isotherms at high relative pressure contain an H3 type hysteresis loop, which suggests that aggregation of plate-like particles cause the formation of nonuniform slit-shaped pores size that are typical of materials with mesopores [33,34].

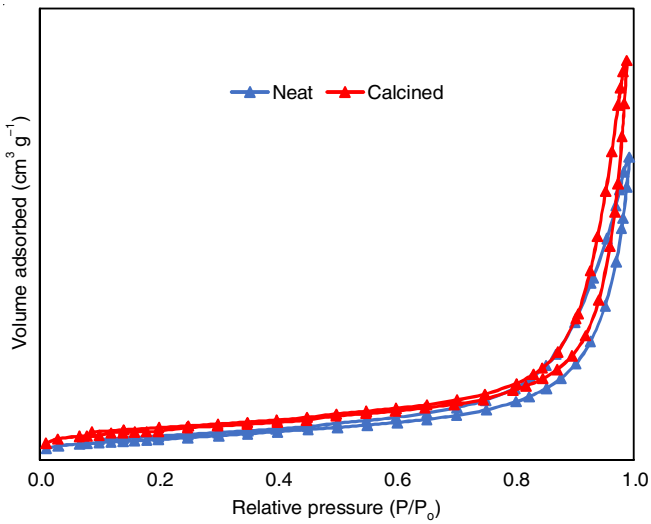

Fig. 5. Isotherm linear plot of neat and calcined MgAl LDH

The BET surface area as well as the corresponding pore volumes and pore size distribution of the prepared MgAl LDH are summarized in Table-5. There was an increase in surface area following the breakdown at 450 ºC, which resulted in the formation of mostly amorphous oxides (MgO and AlO). The surface area for neat and calcined MgAl LDH were 36 and 38 $m^2\ g^{-1}$, respectively. This increase in textural properties has been attributed to the formation of channels and a more open porous network as a result of water vapour and carbonate elimination during decomposition [13]. However, the data show that the surface area of the samples did not change significantly, which contradict with the previous research. This might be due to the improper handling of the materials and also unseen mistake that occur during the preparation of the samples. As a result, it is possible to conclude that the sample preparation process had a significant impact on the textural features of the LDHs.

TABLE-5
BET CHARACTERISTICS OF MgAl LDH
BEFORE AND AFTER CALCINATION

Property	Neat Mg/Al LDH	Calcined Mg/Al LDH
BET surface area ($m^2\ g^{-1}$)	36	38
BJH adsorption (nm)	23	31
BJH desorption (nm)	20	25
Total volume in pores ($cm^3\ g^{-1}$)	0.19	0.23

Conductivity of calcined MgAl LDH in acetonitrile: Conductivity measurement was run with calcined MgAL LDH in acetonitrile as solvent. Calcined MgAl LDH was chosen over neat in this study due to the few favourable properties it has such as enhanced surface area, which is desired when incorporated into electrolyte and eliminate impurities, which is crucial for sustaining the integrity of electrolyte system [35,36]. Table-6 shows the amount of calcined MgAl LDH used and the ionic conductivity (κ) of calcined MgAl LDH solutions. It shows that from the table, the κ value increases from 0 to 12.56×10^{-2} μS cm^{-1} when the LDH was added up to 0.80 % (w/v). Upon raising the percent ratio to 10%, the κ value decrease to 2.32×10^{-2} μS cm^{-1}. The optimum κ value was achieved at 12.56×10^{-2} μS cm^{-1} with percent ratio at 0.80 % (0.40 g). This concentration of MgAl LDH gives the highest κ value in the system was then used in the remaining system.

TABLE-6
IONIC CONDUCTIVITY (κ) OF VARIOUS CONCENTRATION
OF CALCINED MgAl LDH IN ACETONITRILE

Percent ratio (w/v)	Mass (g)	Actual mass (g)	10^2 κ (μS/cm)
0.20	0.10	0.1005	2.56
0.40	0.20	0.2012	7.24
0.60	0.30	0.3019	9.04
0.80	0.40	0.4023	12.56
1.00	0.50	0.5032	11.74
2.00	1.00	1.0030	6.74
4.00	2.00	2.0040	4.36
6.00	3.00	3.0060	4.18
8.00	4.00	4.0060	3.72
10.00	5.00	5.0070	2.32

Determination of limiting molar conductivity (Λ_o) value of $LiClO_4$ in MgAl LDH solution: $LiClO_4$ in acetonitrile system behaves as a weak electrolyte, which means that it only partially dissociates into ions in solution. This results in a smaller number of free-moving ions present in the solution, compared to a strong electrolyte which would be fully dissociated. As a result, the solubility of $LiClO_4$ in solutions containing filler such as MgAl LDH may be affected by the presence of filler. Power law has

been implemented to determine the Λ_o values of the electrolyte system at ambient temperature. Theoretically, the suggested power law should follow a linear equation ($y = mx + c$) formula, hence it should be linear for a certain (limited) range of C_{salt}. An analysis of the double-logarithmic plot of κ against C_{salt} for $LiClO_4$ in MgAl LDH solution was performed using the data from Table-7. Fig. 6 shows the double-logarithmic plot of $LiClO_4$ in MgAl LDH solution at 25 ºC plotted by taking the experimental data as presented in Table-7.

TABLE-7
C_{salt}, κ, Log C_{salt} AND Log κ FOR $LiClO_4$ IN MgAl LDH SOLUTION AT 25 °C

InLab® 741 Calibration standard: 84 µS cm^{-1}; Cell constant: 0.085446 cm^{-1}			
10^6 C_{salt} (mol cm^{-3})	10^5 κ (S cm^{-1})	Log C_{salt}	Log κ
100.01	321.00	-3.9999	-2.4935
80.01	279.00	-4.0969	-2.5544
60.01	221.00	-4.2218	-2.6556
40.01	155.00	-4.3979	-2.8097
20.00	75.80	-4.6989	-3.1203
6.00	21.40	-5.2218	-3.6696
4.00	15.30	-5.3979	-3.8153
2.00	6.49	-5.6989	-4.1878
0.80	2.45	-6.0969	-4.6108
0.40	1.29	-6.3979	-4.8887
0.04	0.11	-7.3979	-5.9473

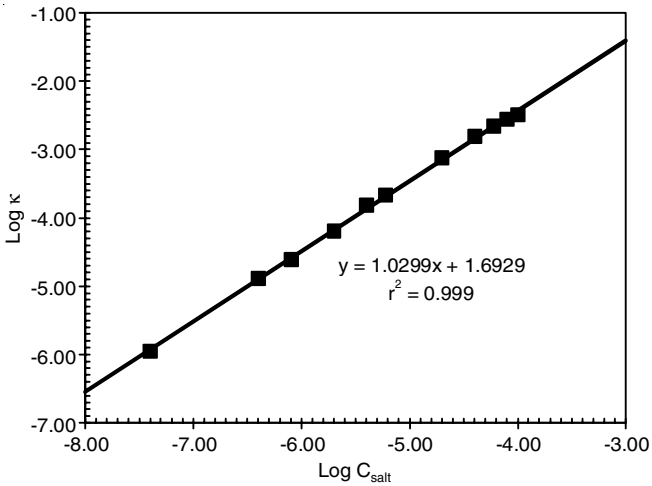

Fig. 6. Double-logarithmic plot of κ *versus* C_{salt} for $LiClO_4$ in MgAl LDH solution at 25 °C

From Fig. 6, the regression function for $LiClO_4$ in MgAl LDH solution at 25 ºC reads:

$$\log \kappa = 1.6929 + 1.0299 \log\left(\frac{C_{salt}}{C^{\theta}}\right) \quad (1)$$

(correlation: 0.9990)

By rearranging eqn. 1, it follows:

$$\kappa = 49.31\left(\frac{C_{salt}}{C^{\theta}}\right)^{1.0299} \quad (2)$$

Thus,

$$\Lambda\ (S\ cm^2\ mol^{-1}) = \frac{49.31}{(C_{salt}/C^{\theta})^{-0.0299}} \quad (3)$$

From the plotted graph, Λ_o value for $LiClO_4$ in MgAl LDH solution was calculated based on eqn. 4:

$$\Lambda_o = K'\gamma C_{ref}^{\gamma-1} \quad (4)$$

where K′ represents the ion mobility and is express as the *y*-axis, while γ is the slope of the logarithm plot.

The Λ_o value was calculated at a fixed salt concentration which is known as reference salt concentration (C_{ref}). The amount of C_{ref} is needed to accurately calculate the Λ_o for an electrolyte system. C_{ref} is approximately half of the lowest C_{salt} that obeys the power law. It is observed that $C_{salt} = 4.0018 \times 10^{-7}$ mol cm^{-3} is the value that obey the power law and was used to estimate C_{ref} for the electrolyte system. Therefore, the amount of C_{ref} for the systems is half of the lowest C_{salt} at $C_{ref} = 2.0009 \times 10^{-7}$ mol cm^{-3}. Hence, the Λ_o value of the above system was calculated after eqn. 4. Thus, by using the relevant parameters (K′ = 49.31 and γ = 1.0299) at $C_{ref} = 2.0009 \times 10^{-7}$ mol cm^{-3} into eqn. 4, the result for quantity Λ_o for $LiClO_4$ in MgAl LDH solution is calculated as below:

$$\Lambda_o = (49.31)(1.0299)(2.0009 \times 10^{-7})^{0.0299} \quad (5)$$

$$\Lambda_o = 32.02\ S\ cm^2\ mol^{-1}$$

The calculated Λ_o value for $LiClO_4$ in MgAl LDH at 25 ºC was found to be 32.02 S cm^2 mol^{-1}. It was observed that the Λ_o value for the electrolyte system decreases as the system is added with filler compared to the system without any filler. This decrease in Λ_o is generally interpreted as a sign that the salt dissociation in the system is improved and the ionic conductivity is enhanced [37]. The addition of a filler to an electrolyte solution can have an impact on the ionic conductivity of the system [38]. Depending on the type of filler and the properties of the electrolyte solution, the addition of a filler may increase or decrease the ionic conductivity of the system. In this case, the addition of filler (MgAl LDH) in the system was found to help enhancing the conductivity of the electrolyte system.

Conclusion

This study aims to investigate the physico-chemical of MgAl layered double hydroxide (LDH), which being synthesized utilizing an alkali free co-precipitation technique. Structure and morphology of the synthesized LDH has been evaluated through many characterization techniques including TGA, PXRD, FTIR, BET and FESEM. The discussion focusses on the neat and calcined MgAl LDH, which demonstrate the structural collapse of hydrotalcite after calcination. The calcination method imparts useful features to the MgAl LDH, which have led to conductivity studies in acetonitrile. The study shows that the optimum electrolytic conductivity (κ) value was achieved at 12.56×10^{-2} µS/cm with percent ratio at 0.80% (0.40 g). This optimal concentration of 0.80 % have been further use in the electrolyte system. The determined limiting molar conductivity (Λ_o) value of $LiClO_4$ in MgAl LDH solution at 25 ºC demonstrated that the κ value increases by one magnitude (from 10^{-9} to 10^{-8}) in the presence of MgAl LDH, which act as filler. In addition, with the presence of filler, the Λ_o value tends to demonstrate a decreasing trend. This indicates that presence of LDH in the system help increase the dissociation of $LiClO_4$ and thus increase the conductivity value.

ACKNOWLEDGEMENTS

The authors express their gratitude to Universiti Teknologi MARA for the support and funding for this project through Grants No. 600-IRMI/FRGS-RACER 5/3 (098/2019) and 600-RMC/GIP 5/3 (125/2023).

CONFLICT OF INTEREST

The authors declare that there is no conflict of interests regarding the publication of this article.

REFERENCES

1. W.J. Kwak, Rosy, D. Sharon, C. Xia, H. Kim, L.R. Johnson, P.G. Bruce, L.F. Nazar, Y.K. Sun, A.A. Frimer, M. Noked, S.A. Freunberger and D. Aurbach, *Chem. Rev.*, **120**, 6626 (2020); https://doi.org/10.1021/acs.chemrev.9b00609
2. M.V. Reddy, A. Mauger, C.M. Julien, A. Paolella and K. Zaghib, *Materials*, **13**, 1884 (2020); https://doi.org/10.3390/ma13081884
3. M. Heishi, H. Niwa, T. Uno, M. Kubo and T. Itoh, *Electrochim. Acta*, **114**, 54 (2013); https://doi.org/10.1016/j.electacta.2013.09.151
4. M. Irfan, M. Atif, Z. Yang and W. Zhang, *J. Power Sources*, **486**, 229378 (2021); https://doi.org/10.1016/j.jpowsour.2020.229378
5. W. Wieczorek, Z. Florjanczyk and J. Stevens, *Electrochim. Acta*, **40**, 2251 (1995); https://doi.org/10.1016/0013-4686(95)00172-b
6. V. Bocharova and A.P. Sokolov, *Macromolecules*, **53**, 4141 (2020); https://doi.org/10.1021/acs.macromol.9b02742
7. M. Sushko and A. Semenov, *J. Mol. Liq.*, **279**, 677 (2019); https://doi.org/10.1016/j.molliq.2019.02.009
8. N. Boaretto, L. Meabe, M. Martinez-Ibañez, M. Armand and H. Zhang, *J. Electrochem. Soc.*, **167**, 070524 (2020); https://doi.org/10.1149/1945-7111/ab7221
9. H. Hanibah, N. Hassan and A. Ahmad, *Asian J. Chem.*, **26**, 4897 (2014); https://doi.org/10.14233/ajchem.2014.16635
10. S.N.A.M. Johari, N.A. Tajuddin, S.K. Deraman and H. Hanibah, *Int. J. Electrochem. Sci.*, **16**, 211049 (2021); https://doi.org/10.20964/2021.10.53
11. M. Daud, A. Hai, F. Banat, M.B. Wazir, M. Habib, G. Bharath and M.A. Al-Harthi, *J. Mol. Liq.*, **288**, 110989 (2019); https://doi.org/10.1016/j.molliq.2019.110989
12. N.A. Tajuddin, J.C. Manayil, A.F. Lee and K. Wilson, *Catalysts*, **12**, 286 (2022); https://doi.org/10.3390/catal12030286
13. E.H Ibrahim, N.A. Tajuddin and N. Hamzah, *Int. J. Eng. Technol.*, **7**, 154 (2019); https://doi.org/10.14419/ijet.v7i4.14.27518
14. N.A. Tajuddin, N.F. Edlina, N. Hamzah, E.H. Ibrahim, *ASM Sci. J.*, **13**, 1 (2020); https://doi.org/10.32802/asmscj.2020.416
15. L. Fan, L. Yang, Y. Lin, G. Fan and F. Li, *Polym. Degrad. Stab.*, **176**, 109153 (2020); https://doi.org/10.1016/j.polymdegradstab.2020.109153
16. E. Conterosito, V. Gianotti, L. Palin, E. Boccaleri, D. Viterbo and M. Milanesio, *Inorg, Chim. Acta*, **470**, 36 (2018); https://doi.org/10.1016/j.ica.2017.08.007
17. N.A. Tajuddin, E.F. Sokeri, N.A. Kamal and M. Dib, *J. Envivorn. Chem. Eng.*, **11**, 110305 (2023); https://doi.org/10.1016/j.jece.2023.110305
18. R. Wijitwongwan, S. Intasa-ard and M. Ogawa, *Chemengineering*, **3**, 68 (2019); https://doi.org/10.3390/chemengineering3030068
19. R. Benhiti, A.A. Ichou, A. Zaghloul, R. Aziam, G. Carja, M. Zerbet, F. Sinan, M. Chiban, *Environ. Sci. Poll. Res. Int.*, **27**, 45767 (2020); https://doi.org/10.1007/s11356-020-10444-5
20. N.A. Tajuddin, J. Manayil, M. Isaacs, C. Parlett, A. Lee and K. Wilson, *Catalysts*, **8**, 667 (2018); https://doi.org/10.3390/catal8120667
21. M.J. Mochane, S.I. Magagula, J.S. Sefadi, E.R. Sadiku and T.C. Mokhena, *Crystals*, **10**, 612 (2020); https://doi.org/10.3390/cryst10070612
22. L. Smoláková, K. Frolich, J. Kocík, O. Kikhtyanin and L. Capek, *Ind. Eng. Chem. Res.*, **56**, 4638 (2017); https://doi.org/10.1021/acs.iecr.6b04927
23. M. Samandari, A.T. Manesh, S.A. Hosseini and S. Mansouri, *J. Water Environ. Nanotech.*, **6**, 72 (2021); https://doi.org/10.22090/jwent.2021.01.007
24. M. Dib, H. Ouchetto, S. Akhramez, H. Fadili, A. Essoumhi, K. Ouchetto, A. Hafid, M. Sajieddine and M. Khouili, *Mater. Today: Proc.*, **22**, 104 (2020); https://doi.org/10.1016/j.matpr.2019.08.106
25. J. Kuljiraseth, A. Wangriya, J.M.C. Malones, W. Klysubun and S. Jitkarnka, *Appl. Catal. B Environ.*, **243**, 415 (2019); https://doi.org/10.1016/j.apcatb.2018.10.073
26. N.I.A. Razak, N.I.S.M. Yusoff and M.U. Wahit, *J. Adv. Res. Exp. Fluid Mechan. Heat Transfer*, **5**, 1 (2021).
27. K. Rybka, J. Matusik, A. Kuligiewicz, T. Leiviskä and G. Cempura, *Appl. Surf. Sci.*, **538**, 147923 (2021); https://doi.org/10.1016/j.apsusc.2020.147923
28. E. Abdollahi, A. Heidari, T. Mohammadi, A. Asadi and M.A. Tofighy, *Sep. Purif. Technol.*, **257**, 117931 (2021); https://doi.org/10.1016/j.seppur.2020.117931
29. L. Yang, J. Chen, Y. Nie, C. Shi and Q. Wang, *J. Environ. Chem. Eng.*, **9**, 105273 (2021); https://doi.org/10.1016/j.jece.2021.105273
30. P. Zhao, D. Gao, H. Zhang, B. Lyu, J. Ma, S.A. Younis and K.H, Kim, *ACS Sustain. Chem. Eng.*, **11**, 11110 (2023); https://doi.org/10.1021/acssuschemeng.3c01681
31. P. Zhang, H. Zhou, Z. Xu, W. Li, Y. Guan and L. Feng, *Inorg. Chem. Comm.*, **150**, 110403 (2023); https://doi.org/10.1016/j.inoche.2023.110403
32. W. Xu, M. Mertens, T. Kenis, E. Derveaux, P. Adriaensens and V. Meynen, *Mater. Chem. Phys.*, **295**, 127113 (2023); https://doi.org/10.1016/j.matchemphys.2022.127113
33. R. Pourfaraj, S.J. Fatemi, S. Y. Kazemi and P. Biparva, *J. Colloid Interface Sci.*, **508**, 65 (2017); https://doi.org/10.1016/j.jcis.2017.07.101
34. L. Jin, Q.J. Huang, H.Y. Zeng, J.Z. Du and S. Xu, *Composites. Part A, Appl. Sci. Manuf.*, **129**, 105717 (2020); https://doi.org/10.1016/j.compositesa.2019.105717
35. A. Farhan, A. Khalid, N. Maqsood, S. Iftekhar, Hafiz, F. Qi, M. Sillanpää and M.B. Asif, *Sci. Total Environ.*, **912**, 169160 (2024); https://doi.org/10.1016/j.scitotenv.2023.169160
36. F. Wang, Z. Wen, Z. Zheng, W. Fang, L. Chen, F. Chen, N. Zhang, X. Liu, R. Ma, G. Chen, *Adv. Energy Mater.*, **13**, 2203830 (2023); https://doi.org/10.1002/aenm.202203830
37. N.Z.N. Hashim, H. Hanibah, I.J. Shamsudin and M.S.Z. Ithnin, *Malaysian J. Chem.*, **25**, 99 (2023); https://doi.org/10.55373/mjchem.v25i4.99
38. S. Hong, Y. Wang, N. Kim and S.B. Lee, *J. Mater. Sci.*, **56**, 8358 (2021); https://doi.org/10.1007/s10853-021-05832-2